TKM Arts College International Journal for Multidisciplinary Research (TIJMR)
Vol. 1 No. 1 June, 2018, Pp 8-14.

Development of Miniaturized High Energy Field Varistors

Anas S[a,b]*, Mangalaraja R V[c] and Ananthakumar S[b]
[a] *Dept. of Chemistry, T.K.M. College of Arts and Science, Kollam, Kerala, India*
[b]*Materials Division, National Institute for Interdisciplinary Science and Technology (CSIR) Trivandrum- 695019, India*
[c] *Department of Materials Engineering, University of Concepcion, Chile*
**Email: anas.tkmchem@gmail.com*

Abstract

This work explains the development of miniaturized high energy field surge arrestors using micro-nano hybrid technologies. Varistor grade nanopowders were first synthesized through a low temperature thermolysis technique. The nanopowders were used as additives to the micron sized commercial varistor powders for obtaining composite varistors. Double stage sintering conditions and microwave aging methods were effectively employed for obtaining dense and fine grained varistors. The structural changes, evolution of microstructures, densification and the electrical properties of these hybrid varistors were thoroughly investigated and assessed using various crystallographic, microscopic and electrical analyses.

Keywords: Miniaturization, Nanopowder, Step-sintering, Hybrid varistors

1. Introduction

Varistors are devices which are mainly used for protecting electrical devices and apparatus from over voltages and variable voltages. Varistor manufacturing is usually based on the conventional solid-state route, where >93mol.% ZnO powder is homogeneously mixed with several metal oxide additives such as Bi, Sb, Co, Cr, Mn, Ni, Ba, Ti and Al [1]. Sintering results the formation of a complex micro structure in varistors in which conducting zinc oxide grains, an electrically insulating secondary spinel phase and a Bi-rich inter granular phase were achieved [2]. Due to such microstructures, the sintered zinc oxide varistors exhibit non-linear current-voltage characteristics and high energy handling capability [3].

Even though the varistor field is extensively studied for the last few decades, in terms of improving the breakdown voltage, grain size control, dopant distribution, finding out the optimal sintering conditions etc.; the current thrust in this field is improving the property of the material without sacrificing the properties and production cost [1-4]. In recent years, the usage of nanopowder for varistor fabrication is coming up in a big way and it is scientifically approved as one of the best method for improving the varistor properties [4-6]. But the nanopowder technologies in varistors are not industrially acceptable due to the economic, toxicity concerns and powder handling difficulties [7]. The leakage current is also high for these nano frame varistors. So in the present study, we have adopted a new strategy of using nanopowder as nano additives to the industrial grade varistor powders for improving its performance. In order to enhance the properties of varistors, we also adopted a step-sintering procedure for the varistor discs in conventional as well as microwave furnaces. The effects of nanofillers by the two sintering methods were finally compared and the results were presented.

2. Experimental

2.1 Materials Used

Zinc nitrate hexahydrate (Merck, 99%), bismuth nitrate (Merck, 99%), cobalt nitrate (CDH, 99%), chromium nitrate (CDH, 98%) and antimony chloride (S.D. fine Chemicals, 98%) were used. Ammonia solution (20%) and nitric acid (16 N) were the other reagents used. Distilled water was used for preparing the solutions.

2.2 Synthesis of Varistor Grade Nanopowders

The varistor composition containing 94 mol% ZnO, 3 mol% Bi_2O_3 and 1 mol% each of Cr_2O_3, CoO and Sb_2O_3, was chosen for the study. The hydrolysis reactions were carried out using ammonium hydroxide solutions (20 vol%). Initially 0.1 M zinc nitrate solution was prepared in distilled water. Appropriate amount of nitrates of cobalt and chromium were dissolved separately in distilled water. Since bismuth nitrate and antimony chloride undergo rapid hydrolysis, their solutions were selectively prepared in HNO_3 (15.8 N). As a first step, zinc nitrate solution was stirred vigorously using a high speed mechanical stirrer and ammonia solution (20 %) was added drop wise. The pH reading of the reactant solution was monitored using a pH meter (Model l pHsystem 362, Systronics) with combined electrode. At pH 6.5, flocculation was noted. Further addition of ammonia solution increased the pH value and the precipitation was completed at pH 8.5. The addition of ammonia was stopped at this pH, but stirring was continued for one more hour and then the precipitate was allowed to settle. The precipitation of dopants were done separately. The hydroxide precipitates were allowed to settle overnight at their respective pH. The hydroxides were washed several times with hot distilled water, finally with alcohol and centrifuged. Then, all hydroxides were taken together and redispersed in appropriate quantity of isopropanol, by mechanical stirring it for one more hour. The stirred slurry was taken in an RB flask fitted with a condenser and refluxed for two hours at 80 ^oC. The product was then transferred and allowed to settle in a 1000 mL beaker. It was then dried in a hot plate and dried in an air oven at 80 ^oC, for 10 hours. Varistors nano powder will be finally obtained with light yellow in color.

2.3 Preparation of Varistor Nanocomposites

Nanocomposites comprising of 10 wt % of nano powder was prepared by ball milling the as prepared nanopowder with industrially processed spray granulated micron sized varistor powders, for 24 hours in water-alcoholic (1:1) media. The powders were dried at 80 ^oC for 10 hours in an air oven. The resultant composite powder was then densified by step-sintering methods.

2.3.1 Step- Sintering

Densification was performed in an electrically heated silicon carbide furnace. 0.6 g powder sample was weighed and uni-axially pressed into small cylindrical discs of diameter 10 mm and thickness 1.5 mm using a hydraulic press. The compacts were pressed at a pressure of 80 MPa. The pellets were then sintered both in conventional and microwave furnaces. In conventional furnace, the heating rate was controlled via. a Libratherm temperature programmer. Initially the temperature was raised to 1100 ^oC and after reaching that point the temperature was minimized rapidly to 850 ^oC and the samples were soaked for 2 hours. The microwave sintering was performed using a 4 kW, 2.45 GHz microwave furnace. An IR-sensor was used for monitoring the sample temperature. The detailed sintering schedules are given in Table1. In all the cases, the furnace was cooled at normal cooling rates. The powder compacts prepared from the doped ZnO powders obtained in the present work, commercial grade varistors powder and nano–micro composite powders were finally sintered at identical conditions to study their comparative properties.

Table 1: Details of heating cycle used for sintering varistor powder

Type of Sintering	**Ramp**
Conventional Step-Sintering	2 $^oC\ min^{-1}$ up to 500 ^oC, 5 $^oC\ min^{-1}$ up to 800 ^oC, 5 $^oC\ min^{-1}$ up to 1100 ^oC, 5 $^oC\ min^{-1}$ up to 850 ^oC; soaking for 3h.
Microwave Step- Sintering	30 $^oC\ min^{-1}$ up to 1100 ^oC, 30 $^oC\ min^{-1}$ up to 850 ^oC; soaking for 30 min.

3. Characterizations

Crystal structure and phase analysis of the products were carried out by powder X-ray diffraction using an X-ray diffractometer (X'PertPro, Philips) with a monochromator on the diffraction beam side (Cu Kα radiation, λ = 0.154nm). The powder samples were mounted as thin layers on a glass substrate and scanning was performed between 2θ angles of 20–60^o. Crystallite size was calculated By Scherer's formula: Crystallite size = 0.9λ/ βcos θ, where λ is the X-ray wavelength, θ the Bragg angle and β line broadening [8-12]. The value of β is usually measured from the increased peak width at half the peak height. The bulk surface area was determined by the Brunauer–Emmett–Teller (BET) technique using a Micromeritics Gemini 2370 instrument operating at the temperature of liquid nitrogen. Degassing of the samples was done at 200 ^{o}C for 2 hours. Transmission electron microscopy images were recorded using a JEOL, 200CX, TEM apparatus. The microstructure analysis of sintered ZnO samples was performed after polishing and thermally etching at 825 ^{o}C. The number of ZnO grains per unit area was determined from SEM micrographs by an image analysis programme. Densities of sintered samples were measured using Archimedes' method. Electrical characteristics of sintered varistors samples were measured by using a Keithley 6517A Electrometer/high resistance meter. From the I–V curves, the breakdown voltage (V_b) and the non-linearity coefficient (α) were determined. α = (log J_2-log J_1)/ (log E_2-log E_1)**,** where E_2 and E_1 are the electric fields at current densities J_2 and J_1 respectively [9-12]. The impedance analysis was performed using HEWLETT 4192A equipment.

4. Results and Discussions

4.1 Nanopowder - Characterization Studies

The X-ray analyses of the powder samples, which are obtained before and after the reflux processes, are presented in Figure.1(a). The diffraction pattern clearly indicates the presence of well crystalline nature of zinc oxide, only for the refluxed samples (80 ^{o}C). The indexed peaks exhibited the phase composition of wurtzite ZnO (hexagonal phase, space group P63mc) (9-11). The peaks can be assigned to (100), (002), (101), (102) and (110) planes, which are in good agreement with the standard JCPDS file for ZnO (No.80-0075). The XRD patterns revealed the presence of randomly oriented ZnO growth units [11-13]. Presence of other minor oxide additives are also confirmed. Peaks corresponding to Bi_2O_3 dopant is also observed. The average crystallite size of ZnO, which are calculated from the maximum intensity peak, using the Debye Scherrer's formula is 21 nm.

Figure 1 (a) Powder X-ray diffraction analysis and (b) TEM image of the varistor nano- powder from alcohol mediated low temperature thermolysis method.

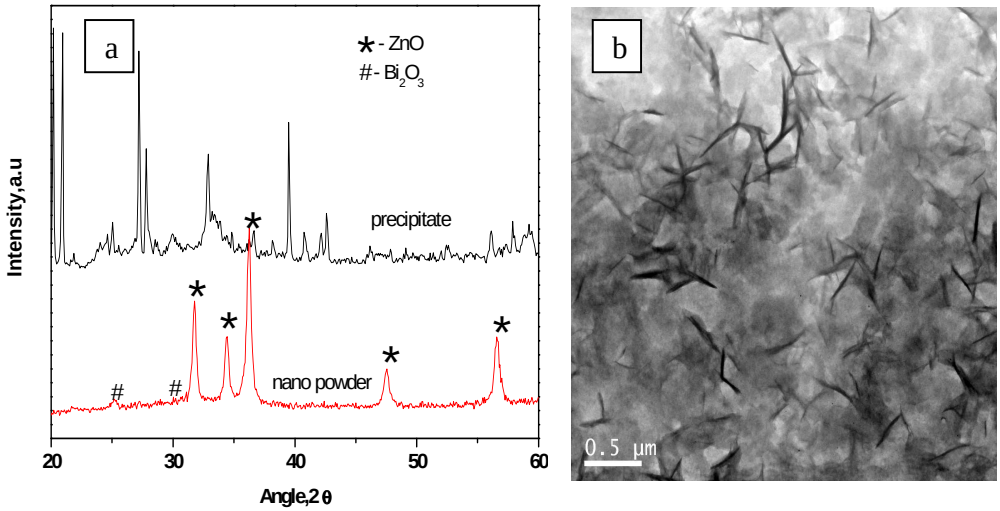

BET surface area is also measured for the nano and micro (conventional) powders. The ZnO varistors grade powder, which are obtained by alcoholic refluxing, possessed a BET surface area of 21 m^2g^{-1}, where as the industrially processed spray granulated micron sized varistor powders exhibited BET surface area of only 2 m^2g^{-1}. The TEM morphological analysis of the refluxed ZnO powder samples (Figure.1(b) revealed the existence of clustered rod-shaped nanostructures. The powder analyzes clearly showed the nano scale regime of the prepared samples. Furthermore, they exhibited uniform size distributions. This again emphasizes the viability of our method as one of the easier method for the large scale synthesis of varistor nanopowders. This could be advantageously used for the design of micro-nano varistors, where the nanofillers can effectively used in the micro varistor powders for their property enhancement. The efficiency of nanopowder in improving the property of the industrially available micron sized powders are thus explored.

4.2 Micro-Nano Varistors- Sintering Studies

Sintering experiments were carried out with the pellets of spray dried industrial micron sized powder (100%), synthesized nanopowder (100%) and a representative composite micro-nano sample (micro with 10% nanopowder additive). Before sintering, green compact of nano powder exhibited pale yellow color and composite has light greenish yellow color. But, after sintering the hue of the nano disc became light brown and that of composite changed to dark green. In order to find out the evolution of varistor phases during sintering, XRD was taken for the representative step-sintered nano powder sample and it is depicted in Figure. 2. XRD patterns shows the peaks for spinel $Zn_7Sb_2O_{12}$ and bismuth rich phase Bi_2O_3, in addition to the major peaks of ZnO [8,12,13].

As shown in table 2, the sintering analysis clearly reveals the high sintered density for the composite samples, both at conventional and microwave conditions. This clearly illustrates the effective packing in nanoadditive added varistor. The morphology of the sintered varistor samples are examined through SEM analysis and the representative images are given in Figure 3.

Figure 2 - Powder X-ray diffraction analysis of step-sintered nanopowder sample.

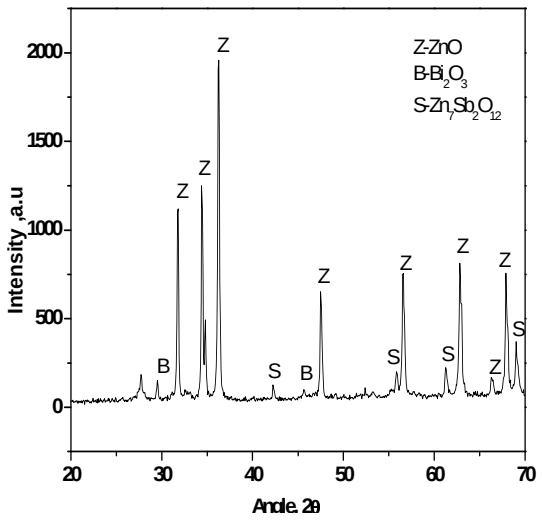

Table 2: Properties of step-sintered and microwave sintered samples

Sample	**Step - sintering**			**Microwave sintering**		
	Density	V_b	α	Density	V_b	α
Micro	5.49	425	17	5.55	386	5
Nano	5.41	452	11	4.63	72	5
Composite	5.57	565	36	5.57	193	22

The SEM analysis clearly showed an average grain size of 8-10 µm for the micro varistor samples. Grain size of 4-5 µm was observed for the nano and 2-4 µm for the composite varistors, respectively. As seen in these images, the number of grains per unit area of the micro-nano composite varistor was found very high when compared to the conventional micro varistor. An effective grain size reduction was observed for these micro-nano samples. This may possibly caused the increased particle packing in these varistors. The influence of nano additive are thus identified as beneficial to the micro sized spray dried powder. Nano sized varistor powders can effectively enter in to the pores of the micron sized grains. In this way the number of grains per unit area could be increased. This would ultimately yield an increase in the non linear current-voltage property. This could be the other reason for the increased density of the micro-nano composite samples.

4.3 High Energy Field Miniaturized Varistors

A comparative study on the performance analysis of the varistors can be done through the non-linear current-voltage characteristics. Varistors are normally characterized by a voltage, which marks the transition from linear to non-linear mode. The voltage at the onset of this nonlinearity, just above the knee of the I-V curve, is the nonlinear voltage which determines the voltage rating of the device [14,15]. The I-V curves are generated by plotting electrical field verses current density values. The performances of the varistors prepared in the present study are depicted in Figure. 4. The density, break down voltage (V_b) and non linearity coefficient (α) of the varistors at the representative sintering conditions are given in Table 2. It is evident from the current–voltage plot of conventionally step-sintered sample that the inclusion of nanopowder to the micron sized powder enhanced the varistors properties to a great extent.

Figure 3 - SEM images of step-sintered varistors (a) micro (b) nano and (c) micro-nano varistors.

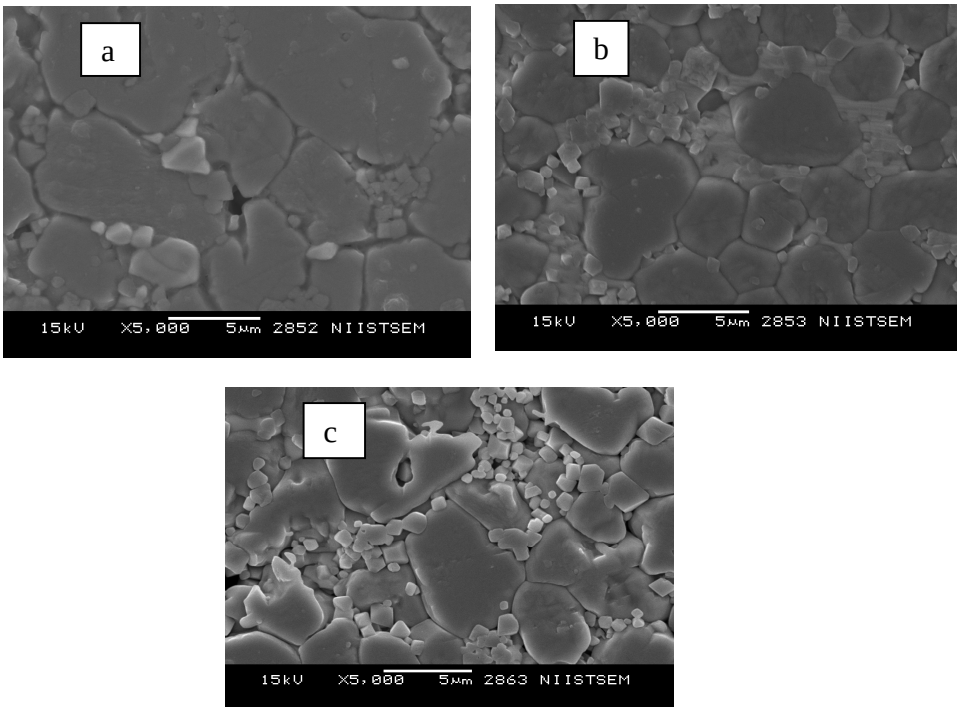

Figure 4 - E-J plot of step-sintered sample in (A) conventional and (B) microwave furnaces. Curve a) Micro b) nano and c) composite varistors.

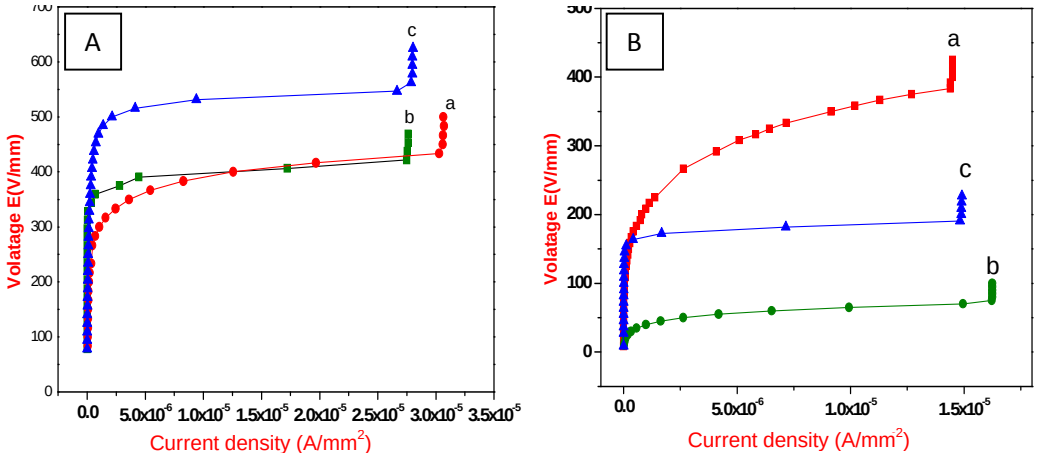

The breakdown voltage as well as non linearity coefficient of composite varistors are much higher than the corresponding micro and nano varistors. This may possibly be due to the effective particle packing, enhanced densification, increased insulating grain boundary volumes. The presence of more number of grains per unit area in micro-nano varistors is an added advantage. These results were further supported by the E-J plot of microwave sintered samples. For these samples, even though break down voltage for composite showed low value than micro varistor, their non linearity coefficient stood higher than the counterparts. The composite varistors showed good varistors property under conventional as well as microwave sintering conditions.

The grain boundary properties of the micro-nano samples were further studied by the impedance spectroscopic analysis (Figure. 5). The analysis of a representative step-sintered micro-nano sample showed the curve corresponding to the resistance from grain boundary. The grain boundary resistance was found to be remarkably good for the micro-nano composites when compared to grain resistance and the electrode resistance. The qualities of a good varistor is thus identified and confirmed in micro-nano varistors via. the impedance analysis. The current study thus provides ample opportunities for developing miniaturized high energy field varistors at low cost, by adopting the micro-nano strategies in varistor technologies.

Figure 5 - Impedance spectra of micro-nano varistors**.**

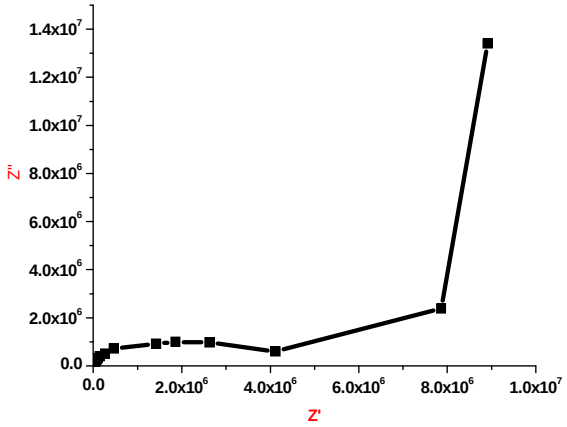

4 Conclusions

Varistor grade nanopowders, with excellent crystallinity, clustered rod like morphology and high surface area; are synthesized through a low temperature themohydrolysis in alcohol media. Micro-nano composite powders are prepared from the nanopowders by effectively utilizing the nanopowder as nanoadditive to the commercially available spray dried micro varistor powders. The densification of the micro, nano and micro-nano powders by step-sintering methods showed specific advantages for conventional and microwave step-sintered varistors. The electrical properties of the varistors revealed that, irrespective of the method of sintering, the micro-nano varistors are capable enough to exhibit high sintered density (>98%) and enhanced non-linear properties (V_b = >550 V/mm, α = >35). This could possibly be achieved in micro-nano varistors, due to the effective particle packing, increased number of grains and grain boundaries; when compared to the micro and nano counterparts. The current study thus foresees ample opportunities for efficient manufacturing of miniaturized high voltage lightning arrestors in a less expensive way, by incorporating the nano-additives to the micro varistors. Miniaturization along with the property enhancement could be possibly be achieved through the nanofillering strategy.

References

[1] T. K. Gupta, J. Am. Ceram. Soc., 73 (1990)181.
[2] H. K. Varma, S. Ananthakumar, K. G. K. Warrier and A. D. Damodaran, Ceram. Int., 22 (1996) 53.
[3] M. A. Kaid and A. Ashour, Appl. Surf. Sci., 253 (2007) 302.
[4] S. Anas, K.V. Mahesh, P. Parsanth, Jobin, S. Ananthakumar, J. Mater. Chem. C, 1 (2013) 6455.
[5] S. C. Pillai, J. M. Kelly, D. E. Mc Cormack and R. Raghavendra, Mater. Sci. Technol., 20, (2004) 964.
[6] D. Mondelaers, G. Vanhoyland, H. Van den Rul, J. D. Haen, M. K. Van Bael, J. Mullens and L. C. Van Poucke, Mat. Res. Bull., 37 (2002) 901.
[7] S. Anas, R. V. Mangalraja, P. Mukundan and S. K. Shukla, Acta Mater., 55 (2007) 5792.
[8] M. Peiteado, J. F. Fernandez and A. C. Caballero, J. Eur. Ceram. Soc., 25 (2005) 2999.
[9] S. C. Pillai, J. M. Kelly, D. E. Mc Cormack and R. Raghavendra, J. Mater. Chem., 18 (2008) 3926.
[10] S. C. Pillai, J. M. Kelly, R. Raghavendra, D. E. Mc Cormack, J. Mater. Chem., 1 (2013) 3268.
[11] W. Mao-Hua, Z. Zhong-Yin, L. Ting-Ting, J. Alloys Comp., 621 (2015) 220.
[12] D. Xu, B. Jiang, L. Jiao, Trans. Nonferrous Met. Soc. China, 22 (2012) 110.
[13] M. J. Maria, S. Balanand, S. Anas, Mater. Des., 92 (2016) 387.
[14] T-T. Liu, M-H. Wang, H-P. Zhang, J. Mater Sci: Mater. Electron., 26 (2015) 9056.
[15] K. V. Mahesh, S. Anas, S. Rahul, S. Ananthakumar, J. Mater. Sci. Mater. Electron., 24 (2013)1495.